IVYSPRING INTERNATIONAL PUBLISHER

*Theranostics*

2018; 8(6): 1607-1623. doi: 10.7150/thno.22958

Research Paper

# Exosomal DMBT1 from human urine-derived stem cells facilitates diabetic wound repair by promoting angiogenesis

Chun-Yuan Chen[1*], Shan-Shan Rao[1,5*], Lu Ren[6], Xiong-Ke Hu[1], Yi-Juan Tan[1], Yin Hu[1,4], Juan Luo[1], Yi-Wei Liu[1,3], Hao Yin[1,4], Jie Huang[1,4], Jia Cao[1], Zhen-Xing Wang[1], Zheng-Zhao Liu[1], Hao-Ming Liu[1], Si-Yuan Tang[6], Ran Xu[7], Hui Xie[1,2,3,4,8]✉

1. Movement System Injury and Repair Research Center, Xiangya Hospital, Central South University, Changsha, Hunan, 410008, China.
2. Hunan Key Laboratory of Organ Injury, Aging and Regenerative Medicine, Changsha, Hunan, China.
3. Department of Sports Medicine, Xiangya Hospital, Central South University, Changsha, Hunan, 410008, China.
4. Department of Orthopedics, Xiangya Hospital, Central South University, Changsha, Hunan, 410008, China.
5. Department of Spine Surgery, Xiangya Hospital, Central South University, Changsha, Hunan, 410008, China.
6. Xiangya Nursing School, Central South University, Changsha, Hunan 410013, China
7. Second Xiangya Hospital, Central South University, Changsha, Hunan 410011, China
8. China Orthopedic Regenerative Medicine Group (CORMed), Changsha, Hunan, China.

* Chun-Yuan Chen and Shan-Shan Rao contributed equally to this work.

✉ Corresponding author: Hui Xie: huixie@csu.edu.cn; #88 Xiangya Road, Changsha, 410008, PR China; Tel: 86-0731-84327068



Received: 2017.09.23; Accepted: 2017.12.12; Published: 2018.02.07

## Abstract

Chronic non-healing wounds represent one of the most common complications of diabetes and need advanced treatment strategies. Exosomes are key mediators of cell paracrine action and can be directly utilized as therapeutic agents for tissue repair and regeneration. Here, we explored the effects of exosomes from human urine-derived stem cells (USC-Exos) on diabetic wound healing and the underlying mechanism.

**Methods:** USCs were characterized by flow cytometry and multipotent differentiation potential analyses. USC-Exos were isolated from the conditioned media of USCs and identified by transmission electron microscopy and flow cytometry. A series of functional assays in vitro were performed to assess the effects of USC-Exos on the activities of wound healing-related cells. Protein profiles in USC-Exos and USCs were examined to screen the candidate molecules that mediate USC-Exos function. The effects of USC-Exos on wound healing in streptozotocin-induced diabetic mice were tested by measuring wound closure rates, histological and immunofluorescence analyses. Meanwhile, the role of the candidate protein in USC-Exos-induced regulation of angiogenic activities of endothelial cells and diabetic wound healing was assessed.

**Results:** USCs were positive for CD29, CD44, CD73 and CD90, but negative for CD34 and CD45. USCs were able to differentiate into osteoblasts, adipocytes and chondrocytes. USC-Exos exhibited a cup- or sphere-shaped morphology with a mean diameter of 51.57 ± 2.93 nm and positive for CD63 and TSG101. USC-Exos could augment the functional properties of wound healing-related cells including the angiogenic activities of endothelial cells. USC-Exos were enriched in the proteins that are involved in regulation of wound healing-related biological processes. Particularly, a pro-angiogenic protein called deleted in malignant brain tumors 1 (DMBT1) was highly expressed in USC-Exos. Further functional assays showed that DMBT1 protein was required for USC-Exos-induced promotion of angiogenic responses of cultured endothelial cells, as well as angiogenesis and wound healing in diabetic mice.

**Conclusion:** Our findings suggest that USC-Exos may represent a promising strategy for diabetic soft tissue wound healing by promoting angiogenesis via transferring DMBT1 protein.

Key words: exosomes, urine-derived stem cells, chronic wound, angiogenesis, DMBT1

## Introduction

Soft tissue injury remains a common occurrence following traumas such as bone fracture [1, 2]. Repair of soft tissue wounds is a well-orchestrated sequence of events involving cell migration, proliferation, extracellular matrix deposition, angiogenesis, and remodeling [3]. In patients with diabetes, the normal wound healing process is impaired and leads to chronic non-healing ulcers, which cause a great burden on patients, their families, society and the healthcare system [3]. A series of multiple mechanisms, including decreased local angiogenesis and diminished blood supply, contribute to delayed wound healing in persons with diabetic ulcers [4]. Thus, strategies designed to augment angiogenic responses in the wound sites may be beneficial for the acceleration of healing of diabetic wounds.

Recently, exosomes, 40-150 nm in diameter extracellular vesicles originating from multivesicular bodies (MVBs), have been of increased interest in regenerative medicine [5]. Exosomes are key mediators of cell paracrine action by transferring genetic materials and proteins to target cells, where the exogenous exosomal molecules can regulate target gene or protein expression and recipient cell function [6, 7]. Accumulating studies have revealed that direct treatment with these nanoparticles can evoke stem cells-like pro-regenerative effects in injured tissues and avoid many risks associated with stem cell transplantation therapy [8, 9]. For skin, exosomes from human adipose-derived mesenchymal stem cells (MSCs) or umbilical cord-derived MSCs or endothelial progenitor cells, upon injection in and around the wound bed of rodent skin wounds, have been found to significantly promote wound healing, collagen synthesis and revascularization of wound sites [8, 10-12]. However, the use of these stem cells is often limited by the source and isolation of stem cells from adipose tissues is invasive. It is imperative to look for a new parent cell source from which it is easy to obtain abundant exosomes for tissue repair.

Zhang and co-workers recently identified a subpopulation of cells isolated from urine possessing MSCs-like biological characteristics, such as cell surface marker expression profiles, self-renewal capacity, multipotent differentiation, pro-angiogenic paracrine effects and immune-modulatory properties [13]. Thus, they termed these cells urine-derived stem cells (USCs) [13]. Compared to other MSCs, USCs have several advantages: 1) USCs can be collected using a simple, safe, non-invasive and low-cost procedure [14]; 2) The isolation of pure USCs is easy and does not require an enzyme digestion process; 3) USCs display high telomerase activity so that they can generate more cells, but not teratomas or tumors [14, 15]; 4) USCs can be obtained regardless of a person's gender, age or health condition (except in those with a urinary tract infection or anuria) [13, 14, 16]. These features make USCs an attractive cell source for generating exosomes. Fu et al. reported that local transplantation of USCs is able to markedly enhance angiogenesis and wound closure in rats [17]. Considering that exosomes are important mediators of cell activity [6, 7], it would be interesting and meaningful to explore whether USCs-derived exosomes (USC-Exos) have the ability to accelerate the healing process of diabetic wounds.

In this study, we determined the effects of USC-Exos on the activities of cultured wound healing-related cells, and profiled the protein expression in USC-Exos and their parent cell USCs to screen the candidate molecules that mediate USC-Exos function. *In vivo*, we verified the effects of USC-Exos on angiogenesis and chronic wound repair in streptozotocin-induced diabetic mice. Meanwhile, the role of the candidate protein in USC-Exos-induced regulation of diabetic wound healing was assessed. Our study aimed to determine the therapeutic benefits of USC-Exos in diabetic wound healing and to elucidate the underlying molecular mechanism.

## Materials and Methods

### Isolation, culture and identification of human USCs

Human urine samples (30–50 mL per sample) were obtained from three healthy donors (two men and one woman) with an age range of 24–28 years. Written informed consent was obtained from all participants and all experimental procedures were approved by the Ethical Review Board at Xiangya Hospital of Central South University (No. 201612653). USCs were isolated from urine samples using a protocol modified from a previous study [18]. Briefly, urine sample was collected in a sterile 50 mL tube containing 500 µL Antibiotic-Antimycotic (100× stock; Gibco, Grand Island, USA). After centrifugation at 400 ×g for 10 min, the supernatant was carefully removed and only 1 mL was left in the tube. The pellets were gently resuspended in the remaining 1 mL urine and 10 mL PBS was added to the fluid. After centrifugation at 200 ×g for 10 min, the supernatant was discarded, leaving only ~0.2 mL plus the pellet. The cell pellet was resuspended in 3 mL primary medium and averagely transferred into three wells of a 12-well plate. All procedures were performed at room temperature. Cells were maintained at 37 °C in a humidified atmosphere containing 5% $CO_2$. 48 h later, 1 mL primary medium was directly added to the culture without removing any medium. Approxima-

tely 96 h after plating, 1 mL medium was removed and 1 mL proliferation medium was added. Thereafter, the whole medium was changed to complete proliferation medium every other day. USC colonies were enumerated by an inverted microscope (Leica DMI6000B, Solms, Germany). Cells were passaged at 80-90% confluence. Early-passage USCs (p2-6) were used for the downstream experiments. Primary medium contains DMEM/F-12 supplemented with the REGM SingleQuot kit (Lonza, USA), 10% fetal bovine serum (FBS; Gibco) and 1% Antibiotic-Antimycotic (Gibco). Proliferation medium contains mixed (1:1 ratio) DMEM/F-12 and RE basal medium (RBM) supplemented with the REGM BulletKit (Lonza), 10% FBS (Gibco), 1% Antibiotic-Antimycotic (Gibco), 1% GlutaMAX (Gibco), 1% NEAA (Gibco), 5 ng/mL bFGF (Peprotech, USA), 5 ng/mL PDGF-BB (Peprotech) and 5 ng/mL EGF (Peprotech).

Multipotent differentiation potentials (including osteogenesis, adipogenesis and chondrogenesis) of USCs were evaluated by using the osteogenic, adipogenic and chondrogenic differentiation media (Cyagen Biosciences, Guangzhou, China) as described previously [17, 19]. Alizarin Red S staining (at day 14), Oil Red O staining (at day 21) and Alcian Blue staining (at day 28) were respectively performed to evaluate the extent of osteogenesis, adipogenesis and chondrogenesis of USCs. The expression of surface marker proteins (including CD29, CD44, CD73, CD90, CD34 and CD45) on USCs was detected by flow cytometry as described previously [8]. Nonspecific fluorescence was determined by incubation of similar cell aliquots with isotype-matched monoclonal antibodies. All antibodies were obtained from BD Biosciences (San Jose, CA, USA).

## Isolation and identification of USC-Exos

After reaching 80% confluence, USCs were washed with PBS and incubated with freshly prepared complete medium containing exosomes-free FBS for 48 h. The conditioned medium of USCs was collected and centrifuged at 300 ×g for 10 min and 2000 ×g for 30 min to remove dead cells and cellular debris. After centrifugation at 10, 000 ×g for 30 min, the supernatant was filtered using a 0.22 μm filter (Millipore, Billerica, USA). 15 mL supernatant was added to an Amicon Ultra-15 Centrifugal Filter Unit (100 kDa; Millipore) and centrifuged at 4000 ×g to about 1 mL. The ultrafiltration liquid was washed twice with PBS and re-ultrafiltrated at 4000 ×g to 1 mL. One-fifth volume of Exoquick Exosome Precipitation Solution (System Biosciences, USA) was added to the ultrafiltration liquid and mixed well by inverting. After incubation for 12 h, the mixture was centrifuged at 1500 ×g for 30 min and the supernatant was removed by aspiration. The exosome pellets were resuspended in 500 μL PBS. All procedures were performed at 4 ºC. The protein content of exosomes was determined by the Pierce BCA Protein Assay Kit (Thermo Fisher Scientific, USA). Exosomes were stored at –80 °C or used for the downstream experiments. The *in vitro* functional properties of USC-Exos were verified by three independent experiments using exosomes from three above-described donors-derived USCs. Proteomics and the effects of USC-Exos on diabetic wound healing were assessed using exosomes from one of the three donors-derived USCs.

Exosomes morphologies were observed by transmission electron microscopy as described previously in detail [20]. Briefly, exosomes suspension was mixed with an equal volume of 4% paraformaldehyde and deposited on Formvar-carbon-coated EM grids. Images were acquired with a Hitachi H-7650 transmission electron microscope (Hitachi, Tokyo, Japan). Exosomal surface marker proteins including CD63 and TSG101 were analyzed by flow cytometry analysis as described previously [21]. Briefly, exosomes were attached to 4 μm aldehyde/sulfate latex beads (Invitrogen, Carlsbad, USA) by mixing 30 μg exosomes in 10 μL beads for 15 min at room temperature. This suspension was diluted to 1 mL with PBS and incubated for an additional 30 min. After termination of the reaction by 100 mM glycine and 2% BSA in PBS, the exosomes-bound beads were washed with 2% BSA in PBS, blocked with 10% BSA and incubated with the primary antibodies anti-CD63 (1:5; Santa Cruz Biotechnology, Santa Cruz, USA) and anti-TSG101 (1:10; ProteinTech, Chicago, USA). 30 min later, the exosomes-bound beads were washed with 2% BSA in PBS and incubated with the Alexa 488-tagged secondary antibodies (1:25; Jackson Immunoresearch, West Grove, USA) for 30 min. Secondary antibody incubation alone served as the negative control. The beads were then washed and analyzed by flow cytometry using a Becton Dickinson FACSscan (San Jose, CA, USA). Results were analyzed with Flowjo software (Tree Star Inc, Ash-land, USA).

## Proteomic analysis

### Preparation of protein samples

USCs (three biological replicate samples called C1, C2 and C3) were seeded in 75 cm2 culture flasks and washed with PBS when they reached 80% confluence. After incubation in fresh exosomes-free complete medium (15 mL per flask) for 48 h, USCs and their conditioned media were collected. Three exosomes samples (E1, E2 and E3) were isolated from the culture medium of C1, C2 and C3, respectively.

The cells and exosomes samples were processed for iTRAQ-based quantitative proteomic analysis by Jingjie PTM BioLab (Hangzhou, China). All samples were sonicated three times on ice in lysis buffer (Sigma-Aldrich, St. Louis MO, USA) and the protein was precipitated with cold 15% trichloroacetic acid for 4 h at –20 °C and then redissolved in a buffer (8 M urea, 100 mM tetraethylammonium bromide (TEAB), pH 8.0). The protein concentration was tested with a 2-D Quant kit (GE Healthcare Bioscience, Shanghai, China). For digestion, the protein solution was reduced with 5 mM dithiothreitol for 30 min at 56 °C, alkylated with 11 mM iodoacetamide for 15 min and diluted by 200 mM TEAB until the urea concentration was below 2 M. Trypsin was then added to the solution at a trypsin-to-protein mass ratio of 1:50 for the first overnight digestion and 1:100 for the second 4 h digestion. Approximately 100 μg protein for each sample was digested with trypsin for the following experiments.

### TMT labeling and HPLC fractionation

After digestion, peptide was desalted by a Strata X C18 SPE column (Phenomenex) and vacuum-dried. Peptide was reconstituted in 1 M TEAB and processed with the 6-plex TMT kit (Sigma). The peptide mixtures were incubated for 2 h and pooled, desalted and dried by vacuum centrifugation. Then, the sample was fractionated by high pH reverse-phase HPLC using an Agilent 300 Extend C18 column (5 μm particles, 4.6 × 250 mm). Peptides were separated with a gradient of 2% to 60% acetonitrile in 10 mM ammonium bicarbonate pH 9.0 over 80 min into 80 fractions and then combined into 18 fractions and dried by vacuum centrifuging.

### Quantitative proteomic analysis by LC-MS/MS

Peptides were dissolved in 0.1% formic acid, desalted in a reversed-phase pre-column (Acclaim PepMap 100; Thermo) and separated using a reversed-phase analytical column (Acclaim PepMap RSLC; Thermo). The gradient was comprised of an increase from 7% to 25% solvent B (0.1% FA in 98% ACN) over 24 min, 25% to 40% in 8 min and climbing to 80% in 4 min then holding at 80% for the last 4 min, all at a constant flow rate of 350 nL/min on an EASY-nLC 1000 UPLC system. Peptides were subjected to NSI source followed by tandem mass spectrometry (MS/MS) in Q Exactive TM (Thermo) coupled online to the UPLC. Intact peptides were detected in the orbitrap at a resolution of 70,000. Peptides were selected for MS/MS using a NCE setting of 28; ion fragments were detected in the orbitrap at a resolution of 17,500. A data-dependent procedure that alternated between one MS scan followed by 20 MS/MS scans was applied for the top 20 precursor ions above a threshold ion count of $1 \times 10^4$ in the MS survey scan with 30.0 s dynamic exclusion. The electrospray voltage applied was 2.0 kV. Automatic gain control was used to prevent overfilling of the orbitrap and $5 \times 10^4$ ions were accumulated for generation of MS/MS spectra. For MS scans, the $m/z$ scan range was 350 to 1800. Fixed first mass was set as 100 $m/z$.

### Database search and bioinformatics analysis

The resulting MS/MS data was processed using MaxQuant with integrated Andromeda search engine (v.1.5.2.8). Tandem mass spectra were searched against swissprot Human database. Trypsin/P was specified as cleavage enzyme allowing up to 2 missing cleavages. Mass error was set to 10 ppm for precursor ions and 0.02 Da for fragment ions. Carbamidomethyl on Cys was specified as a fixed modification and oxidation on Met and acetylation on the protein N-terminus were specified as variable modifications. For the protein quantification method, TMT 6-plex was selected in Mascot. The false discovery rate (FDR) was adjusted to < 1% at protein, peptide and PSM levels.

Gene Ontology (GO) analysis was performed to classify all identified proteins into three categories (cell component, molecular function and biological process) using the UniPort-GOA database (http://www.ebi.ac.uk/GOA/), InterProScan (http://www.ebi.ac.uk/interpro/) and GO annotation (http://geneontology.org/). Differentially expressed proteins were identified with a cutoff of absolute fold change ≥ 1.5. For each category, a two-tailed Fisher's exact test was employed to test the enrichment of the differentially expressed protein against all identified proteins. The GO with a corrected $p$ value < 0.05 was considered significant.

## Inhibition of deleted in malignant brain tumors 1 (DMBT1)

Three lentivirus shRNAs (shDMBT1 #1, shDMBT1 #2 and shDMBT1 #3) and the scramble control shRNA (Con shRNA) were obtained from Cyagen Biosciences (Guangzhou, China) and the virus packaging was performed by Cyagen Biosciences. Cell transfection was performed following the handbook from the manufacturer. In brief, the cells were incubated in retroviral supernatant supplemented with 10 μg/mL polybrene (Cyagen). 24 h later, the medium was changed to fresh complete medium. 72 h after infection, the cells were selected with 2.5 μg/mL puromycin (Sigma) in the culture medium. The shRNA sequences used in this study were the following: shDMBT1 #1:

5'-ACCTTGAGGTTGGTCAATTTACTCGAGTAAATTGACCAACCTCAAGGT-3'; shDMBT1 #2: 5'-CCCGTCCAAACACAGATTATTCTCGAGAATAATCTGTGTTTGGACGGG-3'; shDMBT1 #3: 5'-TCCGTGTACCTGCGTTGTAAACTCGAGTTTACAACGCAGGTACACGGA-3'; Con shRNA: 5'-CCTAAGGTTAAGTCGCCCTCGCTCGAGCGAGGGCGACTTAACCTTAGG-3'.

## Culture of keratinocytes, fibroblasts and endothelial cells

Human skin keratinocytes HaCaT (FuHeng Biology, Shanghai, China) and human skin fibroblasts (HSFs; FuHeng) were cultured in high-glucose Dulbecco's modified eagle medium (Gibco) supplemented with 10% FBS. Human microvascular endothelial cells (HMECs; Cell Bank of the Chinese Academy of Sciences, Shanghai, China) were cultured in MCDB131 medium (Gibco) containing 10% FBS, 1 μg/mL hydrocortisone (Sigma), 1% GlutaMAX (Gibco) and 10 ng/mL epidermal growth factor (Sigma). Cells were incubated at 37 °C, 5% CO2.

## Exosomes uptake assay

USCs were labeled with a green fluorescent dye (PKH67; Sigma) according to the manufacturer's instructions. Then, the cell-labeled suspension was centrifuged at 300 ×g for 15 min and the supernatant was discarded. Cells were washed twice with PBS and seeded into culture flasks for 48 h of incubation. Next, USC-Exos were isolated from the conditioned media of USCs and incubated with skin cells at 37 °C for 3 h. Cells were then washed with PBS and fixed with 4% paraformaldehyde for 15 min. After washing with PBS, nuclei were stained with DAPI (0.5 μg/mL; Invitrogen, Carlsbad, USA). The signals were analyzed with a fluorescence microscope (Leica DMI6000B, Solms, Germany).

## *In vitro* effects of USC-Exos on skin cells

For testing the effects of USC-Exos on the activities of skin cells (HaCaT, HSFs and HMECs), the cells were incubated in their respective culture medium and received different treatments: 1) control group (treated with an equal volume of exosomes diluent (PBS)); 2) USC-Exos group (treated with 100 μg/mL USC-Exos). For testing the role of DMBT1 in USC-Exos-induced regulation of the activities of endothelial cells, HMECs were cultured in MCDB131 medium under different treatment conditions: 1) control group (treated with PBS); 2) $USCs^{Con\ shRNA}$-Exos group (treated with 100 μg/mL exosomes from Con shRNA-transfected USCs); 3) $USCs^{shDMBT1\ \#1}$-Exos group (treated with 100 μg/mL exosomes from DMBT1-silenced USCs).

### Proliferation assay

In brief, cells (5 × $10^3$ cells per well; four replicates per group) were seeded into 96-well culture plates and treated with exosomes (100 μg/mL) from different groups or PBS. A group without cells served as the blank. On days 1, 2, 3, 4, and 5, cell counting kit-8 reagent (CCK-8; 10 μL per well; 7Sea Biotech, Shanghai, China) was added to the culture medium (100 μL per well). After incubation at 37 °C for 3 h, the absorbance of each well was measured at 450 nm by a microplate reader (Bio-Rad 680, Hercules, USA) and cell proliferation was represented through the mean absorbance of each individual well minus the blank value.

### Scratch wound healing assay

Cells (2 × $10^5$ cells per well; three replicates per group) were seeded into a 12-well plate and incubated at 37 °C. After the cells had attached, the monolayer was scratched with a p200 pipette tip, washed with PBS to remove floating cells and then exposed to exosomes (100 μg/mL) from different groups or an equal volume of PBS. Mitomycin-C (5 μg/mL; Sigma) was present throughout the migration assays to exclude the influence of cell proliferation on wound closure. HaCaT and HSFs were photographed at 0 h, 12 h and 24 h later; HMECs were photographed at 0 h, 6 h and 12 h after wounding. The rate of migration area was calculated as the ratio of closure area to initial wound as described previously [8]: Migration area (%) = $(A_0 - A_n)/A_0 \times 100$, where $A_0$ represents the area of initial wound area and $A_n$ represents the remaining area of wound at the metering point.

### Transwell migration assay

Boyden chamber assays were performed using 24-well transwell inserts (Corning, NY, USA) with 8 μm pore-sized filters and 24-well culture plates as described previously [22, 23]. Cells (1 × $10^4$ cells per well; three replicates per group) were suspended in low serum (5% FBS) medium and plated into the upper chamber. 500 μL complete medium (containing 10% FBS) supplemented with exosomes (100 μg/mL) from different groups or an equal volume of PBS was added to the lower chamber. After incubation for 12 h, cells attached to the upper surface of the filter membranes were removed by cotton swabs and cells on the bottom side of the filter (the migrated cells) were stained with 0.5% crystal violet for several minutes. The number of migrated cells was quantified under an optical microscope at a ×100 magnification (Leica).

### Tube formation assay

50 μL cold Matrigel per well was transferred into

each well of a 96-well plate and incubated at 37 °C for 30 min. Then, HMECs (2 × $10^4$ cells per well; three replicates per group) were plated into the Matrigel-coated 96-well plates and treated with exosomes (100 μg/mL) from different groups or PBS. 6 h after seeding, tube formation was detected under an inverted microscope (Leica). The indicators (total branching points, total tube length and total loops) revealing the abilities to form tubes were measured by using Image-Pro Plus 6.0 software.

### Quantitative real-time PCR (qRT-PCR) analysis

Total RNA was extracted using TRIzol Reagent (Invitrogen, Carlsbad, USA) and 1 μg total RNA from each sample was reverse transcribed into cDNA with a Revert Aid First Strand cDNA Synthesis kit (Fermentas, Burlington, Canada). qRT-PCR was performed using FastStart Universal SYBR Premix ExTaq (Takara Biotechnology, Japan). Reactions were processed and analyzed on an ABI PRISM® 7900HT System (Applied Biosystems, USA). Relative gene expression was calculated using the $2^{-\Delta\Delta CT}$ method and GAPDH was used as a housekeeping gene for normalization. Primer sequences used for qRT-PCR were as follows: h-DMBT1: forward, 5'-GCCAACCTC TCGTGCATCAA-3', and reverse, 5'-TGTCCCAGTAG TCATCACACAC-3'; h-Gapdh: forward, 5'-ATCCCA TCACCATCTTCC-3', and reverse, 5'-GAGTCCTTCC ACGATACCA-3'.

### Western blotting

Lysates of cells or exosomes were diluted at a ratio of 1:5 with protein loading buffer (5×; Beyotime Biotechnology, Jiangsu, China) and heated at 95 °C for 5 min. Protein extracts were separated by SDS-PAGE (6% gel for DMBT1 and 12% gel for other proteins) and transferred to polyvinylidene fluoride membranes (Immobilon P, Millipore, USA). The membranes were blocked with 5% milk in TBST (Tris-buffered saline, 10 mM Tris-HCl pH 7.5, 150 mM NaCl, 0.1% Tween-20) for 60 min at room temperature, incubated with primary antibodies at 4 °C overnight and then incubated with the horseradish peroxidase-conjugated secondary antibodies at 37 °C for 1 h. Primary antibodies and dilutions were used as follows: anti-CD9 (1:500; Santa Cruz), anti-CD63 (1:300; Santa Cruz), anti-CD81 (1:500; Santa Cruz), TSG101 (1:1000; ProteinTech, Chicago, USA), anti-DMBT1 (1:5000; Abcam, Cambridge, Britain), anti-VEGF-A (1:500; R&D system, Minneapolis, USA), Akt (1:500; Cell Signaling Technology, Danvers, USA), anti-phosphorylate Akt (p-Akt; 1:500; Cell Signaling Technology) and anti-GAPDH (1:5000; Cell Signaling Technology). All the secondary antibodies (1:5000) were obtained from Cell Signaling Technology. The immunoreactive bands were visualized using enhanced chemiluminescence reagent (Thermo Fisher Scientific, Waltham, USA) and imaged by the ChemiDoc XRS Plus luminescent image analyser (Bio-Rad).

### Mouse skin wound model and treatments

Animal care and experimental procedures were approved by the Laboratory Animal Management Committee of Xiangya Hospital of Central South University (No. 201612654). Forty female C57BL/6 mice (3-months-old and weighing 25-30 g) were used in the present study. Experimental diabetes was induced by intraperitoneal injection of streptozotocin (STZ; 50 mg/kg; Sigma) freshly dissolved in a 0.1 M phosphate-citrate buffer (pH 4.5) for 5 consecutive days for the fasted (18 h) mice [24], whereas control mice (non-DM control; n=6) received only citrate buffer. Blood glucose levels were monitored after 3 days and those mice (n > 30) showing blood glucose levels greater than 16.67 mM were diagnosed as diabetic. The diabetic mice were kept under observation for two weeks before creation of skin wounds.

Thirty diabetic mice were selected and anesthetized by intraperitoneal injection of 50 mg/kg pentobarbital sodium (Sigma). After shaving the mice, two full-thickness excisional skin wounds (6 mm in diameter) were created on the upper back of each mouse. Then, the mice were randomly divided into three treatment groups: 1) PBS group (wounds treated with 100 μL PBS); 2) $USCs^{Con\ shRNA}$-Exos group (wounds treated with 200 μg $USCs^{Con\ shRNA}$-Exos in 100 μL PBS); 3) $USCs^{shDMBT1\ \#1}$-Exos group (wounds treated with 200 μg $USCs^{shDMBT1\ \#1}$-Exos in 100 μL PBS). Briefly, the mice were subcutaneously injected with $USCs^{Con\ shRNA}$-Exos, $USCs^{shDMBT1\ \#1}$-Exos or PBS around the wounds at 4 injection sites (25 μL per site). At days 0, 6, 9 and 12 post-wounding, the wounds were photographed and measured with a caliper rule. Wound-size reduction was calculated using the equation: wound-size reduction (%) = $(A_0 - A_t)/A_0 \times 100$, where $A_0$ is the initial wound area, and At is the wound area at the indicated times. 12 days after the operation, the mice were sacrificed and skin samples were harvested. The undersurface of the skin was viewed and photographed to detect the newly formed blood vessels.

### Histological and immunofluorescence analysis

The skin specimens containing the wound bed and surrounding healthy skin were fixed in 4% paraformaldehyde, dehydrated with a series of graded ethanol, embedded in paraffin and then cut

into 10 μm thick sections. For histological analysis, wound sections were stained with hematoxylin and eosin (H&E) and the percentage of re-epithelialization (E%) was assessed as described previously [8]: E% = Wn/Wo × 100, where Wo is the original wound area, and Wn is the length of newly generated epithelium across the surface of the wound. Masson's trichrome staining was used to evaluate the degree of collagen maturity. The mean staining intensity for Masson was measured in at least three random visual fields per section using Image-Pro Plus 6 software. For immunofluorescence staining for ki67 and CD31, the sections were rehydrated and heated in a microwave in citrate buffer (0.01 M; pH 6.0) for 15 min to retrieve the antigen. The sections were then blocked in 1% BSA for 30 min at room temperature, incubated with the primary antibodies anti-ki67 (1:100; Abcam) or anti-CD31 (1:50; Abcam) overnight at 4°C, and then incubated with the respective secondary antibodies (1:250; Abcam) at room temperature for 1 h while avoiding light. Images were acquired with a fluorescence microscope (Leica). Vessel density and ki67-postive cells were quantified from at least three random visual fields per section using Image-Pro Plus 6 software.

### Statistical analysis

Data are presented as mean ± standard deviation (SD). Statistical analysis of multiple-group comparisons was analyzed by one-way analysis of variance (ANOVA), followed by the Bonferroni *post hoc* test to assess the significance of differences between two groups. Analyses were performed using GraphPad Prism software. Differences were judged to be statistically significant when $P < 0.05$.

## Results

### Identification of USCs and USC-Exos

USC colonies appeared approximately 3 and 7 days after initial plating. The cells exhibited a spindle-like morphology (**Fig. 1A**). When cultured in osteogenic, adipogenic or chondrogenic medium, USCs were able to differentiate into osteoblasts, adipocytes or chondrocytes, as evidenced by Alizarin Red S staining (**Fig. 1B-a**), Oil Red O staining (**Fig. 1B-b**) and Alcian Blue staining (**Fig. 1B-c**), respectively. Flow cytometry analysis revealed that USCs were highly positive for MSC surface markers including CD29, CD44, CD73 and CD90, but negative for CD34 and CD45 (**Fig. 1C**). All these features were consistent with the findings of previous studies [13-15, 17]. Transmission electron microscopy and flow cytometric analysis were used to identify the nanoparticles derived from USCs. As shown in **Fig. 1D-E**, the vesicles exhibited a cup- or sphere-shaped morphology with a mean diameter of 51.57 ± 2.93 nm, similar to previously described exosomes [5]. Flow cytometric analysis showed the presence of exosomal markers including CD63 and TSG101 (**Fig. 1F**), which further confirmed their identity as exosomes.

### USC-Exos promote the proliferation and migration of keratinocytes and fibroblasts

Keratinocytes and fibroblasts play important roles in wound healing [25]. To examine the effects of USC-Exos on keratinocyte and fibroblast function, we firstly determined whether USC-Exos could be internalized into these cells. As shown in **Fig. 2A**, the green fluorescent dye (PKH67)-labeled USC-Exos were transferred to the perinuclear region of the human keratinocytes cell line HaCaT and skin fibroblasts (HSFs) after 3 h incubation. For functional assays, HaCaT and HSFs were treated with USC-Exos or an equal volume of PBS for the indicated times. CCK-8 analysis was applied to measure the effect of USC-Exos on proliferation of HaCaT and HSFs. The results showed that the proliferation of these cells was markedly elevated in response to exosomes stimulation (**Fig. 2B**). USC-Exos treatment also caused a remarkable increase in HaCaT and HSFs migration compared to control groups, as evidenced by the scratch wound assay (**Fig. 2C-D**) and transwell migration assay (**Fig. 2E-F**). These data suggest that the activation of keratinocytes and fibroblasts may contribute to the effects of USC-Exos on wound healing.

### USC-Exos enhance the angiogenic activities of endothelial cells

We then assessed the impact of USC-Exos on the angiogenic activities of endothelial cells. Fluorescence microscopy analysis revealed that PKH67-labeled USC-Exos were incorporated into human micro-vascular endothelial cells (HMECs) (**Fig. 3A**). The tube formation assay on Matrigel is an *in vitro* model of angiogenesis. As shown in **Fig. 3B**, HMECs treated with USC-Exos showed a higher number of capillary-like structures compared with the control group. Quantitative measurements revealed that the total tube length, total branching points and total loops were all significantly increased after USC-Exos stimulation (**Fig. 3C**). CCK-8 assay showed that HMECs exhibited a much stronger proliferative ability when exposure to USC-Exos (**Fig. 3D**). Transwell assay (**Fig. 3E-F**) and scratch wound healing assay (**Fig. 3G-H**) revealed that exosomes remarkably up-regulated the motility of HMECs. These findings indicate that USC-Exos augment the angiogenic activities of endothelial cells.

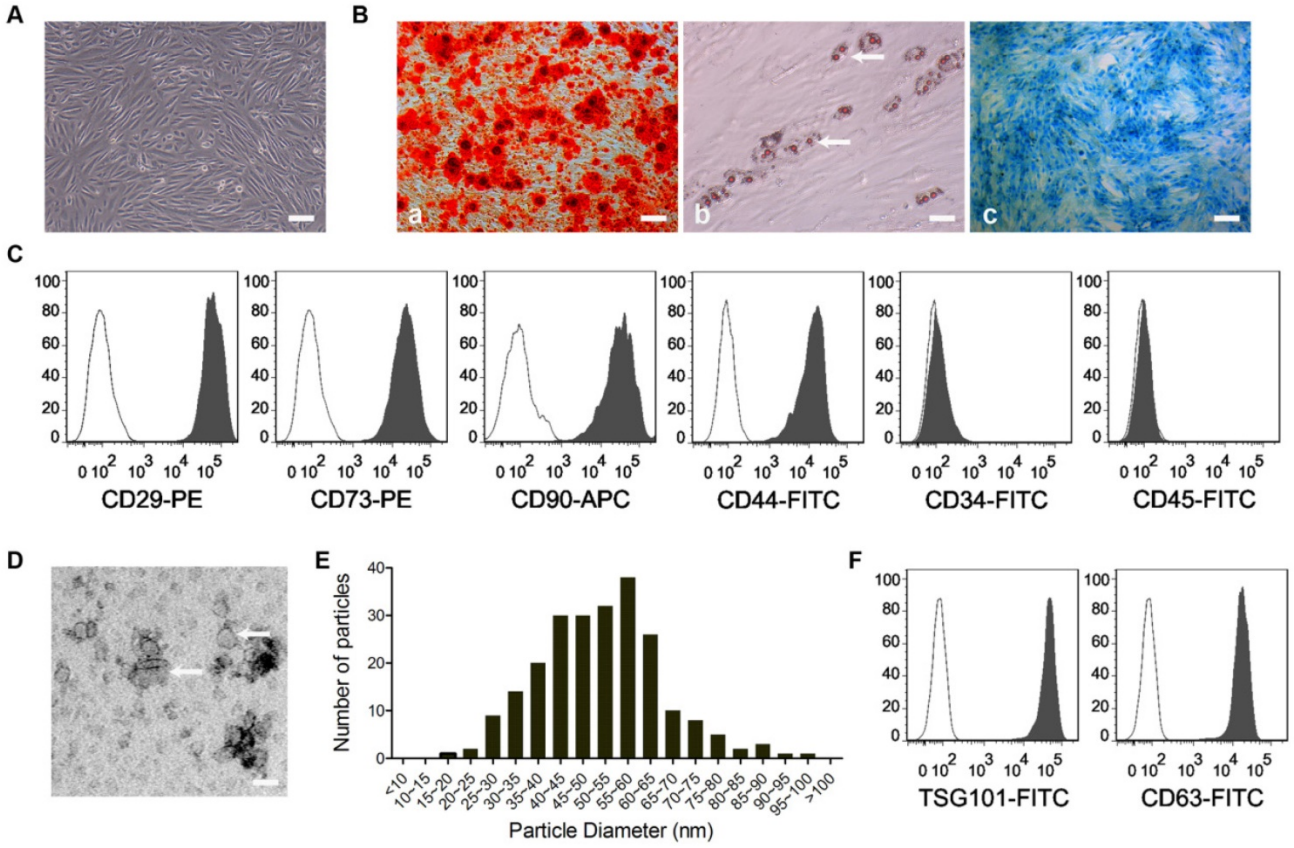


**Figure 1. Identification of USCs and USC-Exos. (A)** USCs showed a spindle-like morphology. Scale bar: 100 μm. When cultured in osteogenic, adipogenic or chondrogenic medium, USCs were able to differentiate into osteoblasts, adipocytes or chondrocytes, as evidenced by Alizarin Red S staining (**B-a;** Scale bar: 100 μm), Oil Red O staining (**B-b;** Scale bar: 50 μm) and Alcian Blue staining (**B-c;** Scale bar: 100 μm), respectively. White arrows indicate lipid droplets. **(C)** Flow cytometry analysis of the cell surface markers on USCs. The isotype controls are illustrated as blank curves and the test samples are illustrated as solid gray curves. **(D)** Morphology of USC-Exos under transmission electron microscopy. Scale bar: 50 nm. White arrows indicate exosomes. **(E)** The mean diameter of USC-Exos (51.57 ± 2.93 nm; n=232) was calculated from TEM images and the exosomes frequency was plotted for indicated size groups of 5 nm each. **(F)** Representative flow cytometry histograms showing the presence of exosomal surface markers CD63 and TSG101 on USC-Exos-bound beads (solid gray curves). Secondary antibody incubation alone served as the negative control (blank curves).

## Proteomic analysis of USCs and USC-Exos

To investigate the functional molecules that mediate the effects of USC-Exos, proteomic analysis using ITRAQ technology was conducted to detect the protein expression profiles in USC-Exos and their parent cell USCs. In total, 4214 protein groups were identified, among which 3762 proteins were quantified. GO analysis was conducted to classify all identified proteins in three categories, including cell component, molecular function and biological process (data not shown). Differentially expressed proteins were identified with a cutoff of absolute fold change ≥ 1.5 and $p$ value < 0.05. The results showed that 2911 proteins were differentially expressed between USC-Exos and USCs. Among them, 442 proteins in USC-Exos were significantly higher and 2469 proteins were much lower than in their parent cell USCs. All proteins identified and quantified in USC-Exos and USCs are listed in the **Table S1**. Then, the differentially expressed proteins were biologically interpreted and their involved biological processes were explored (**Fig. S1**). The results revealed that USC-Exos were highly enriched in the proteins that are involved in regulation of multiple biological processes related to wound healing, such as skin cell proliferation, migration and differentiation, angiogenic tubule formation and vascular development, extracellular matrix assembly and organization, response to wounding and external stimulus, as well as cytokine production (**Fig. 4A**). **Fig. 4B** shows the ratio of expression of a class of angiogenesis-related proteins and exosomal markers in USC-Exos compared to that in USCs. The data showed that DMBT1, a potent promoter of angiogenesis [26], was up-regulated 137.42 ± 16.99-fold in USC-Exos as compared to USCs. VEGF-A, a major positive regulator of both physiological and pathological angiogenesis [27, 28], was also enriched in USC-Exos (E/C=16.44 ± 0.96-fold). Results of western blotting confirmed the enrichment of DMBT1 and VEGFA in USC-Exos (**Fig. 4C**). The protein levels of exosomal

markers including CD9, CD63, CD81 and TSG101 were also verified by western blotting. Data revealed that USC-Exos had much higher levels of CD9 and CD81, a comparable level of TSG101, and a lower level of CD63 compared to USCs, all of which were consistent with the proteomic data.

## DMBT1 mediates the pro-angiogenic effects of USC-Exos on endothelial cells

To investigate the role of DMBT1 in USC-Exos-induced pro-angiogenic effects on endothelial cells, three shRNAs (shDMBT1 #1, shDMBT1 #2 and shDMBT1 #3) were used to knockdown the expression of DMBT1 in USCs and the inhibitory efficiency of these shRNAs was tested by qRT-PCR (**Fig. 5A**). USCs transfected with the shRNA showing the highest inhibitory efficiency (shDMBT1 #1) or with the scramble control shRNA (Con shRNA) were used as a "factory" to generate exosomes for downstream assays. Results of western blotting determined the down-regulation of DMBT1 in exosomes from DMBT1-silenced USCs ($USCs^{shDMBT1\ \#1}$-Exos) (**Fig. 5B**). CCK-8 assay showed a decreased ability of USC-Exos to promote the proliferation of HMECs when DMBT1 was knocked down in their parent cell USCs (**Fig. 5C**). As evidenced by the scratch wound healing assay (**Fig. 5D-E**) and the transwell assay (**Fig. 5F-G**), the pro-migratory effects of USC-Exos were also suppressed once DMBT1 content was reduced in USC-Exos. Tube formation assay showed fewer numbers of capillary-like structures on Matrigel by HMECs treated with $USCs^{shDMBT1\ \#1}$-Exos compared with the $USCs^{Con\ shRNA}$-Exos group (**Fig. 5H**). Quantitative analysis of the total tube length, total branching points and total loops further confirmed that down-regulation of DMBT1 in USC-Exos blocked their positive effects on tube formation (**Fig. 5I-K**). Studies have reported that DMBT1 is able to increase the expression of VEGF-A [29] and activate the PI3K-Akt pathway [30]. Thus, we performed western blotting to detect the levels of VEGF-A, Akt and p-Akt in HMECs following treatment with $USCs^{shDMBT1\ \#1}$-Exos, $USCs^{Con\ shRNA}$-Exos or an equal volume of PBS for 24 h. As shown in **Fig. 5L**, the ability of USC-Exos to induce VEGF-A expression and phosphorylation of Akt was markedly compromised when DMBT1 expression in USC-Exos was inhibited. Collectively, our findings suggest that DMBT1 is required for USC-Exo-induced promotion of endothelial angiogenesis.

## Exosomal DMBT1 accelerates cutaneous wound healing in diabetic mice

To determine the effects of USC-Exos on diabetic wound healing and the role of DMBT1 in this process, diabetic mice were established by injection of STZ and two full-thickness cutaneous wounds were created on the back of each mice, followed by subcutaneous injection of $USCs^{shDMBT1\ \#1}$-Exos, $USCs^{Con\ shRNA}$-Exos or an equal volume of PBS. Digital photographs of wounds showed much faster wound closure in diabetic mice exposed to $USCs^{Con\ shRNA}$-Exos, as determined by smaller wound areas measured at days 6, 9, and 12 post-wounding when compared with the control (PBS) group (**Fig. 6A-B**). However, the pro-wound healing effect was markedly decreased with the inhibition of DMBT1 expression in USCs-Exos (**Fig. 6A-B**). H&E staining was carried out to evaluate the extent of re-epithelialization and scar formation. As shown in **Fig. 6C**, much longer newly formed epidermis and dermis with hair follicles and fat cells were observed in the wounds treated with $USCs^{Con\ shRNA}$-Exos, as compared with the PBS-treated wounds at day 12 after operation. Quantitative measurements confirmed that $USCs^{Con\ shRNA}$-Exos-treated wounds had a higher rate of re-epithelialization and a lower level of scar formation than the control group (**Fig. 6D**). However, when compared with the $USCs^{Con\ shRNA}$-Exos group, the beneficial effect on re-epithelialization and the inhibitory effect on scarring in the $USCs^{shDMBT1\ \#1}$-Exos group were attenuated. Histological analysis of Masson's trichrome-stained sections showed larger amounts of wavy collagen fibers in $USCs^{Con\ shRNA}$-Exos-treated wounds compared to the control group, but the ability of $USCs^{shDMBT1\ \#1}$-Exos to promote collagen synthesis was not obvious (**Fig. 6E**). Quantification of the mean intensity of Masson-stained areas further confirmed the efficiency of USC-Exos in promoting collagen deposition and the critical role of DMBT1 in this process (**Fig. 6F**). We also performed ki67 staining to test the proliferation of skin cells in the wound sites. The result revealed that ki67-positive cells were rarely observed in the PBS-treated wounds at day 12 after operation, while larger numbers of proliferating skin cells appeared in the wounds transplanted with $USCs^{Con\ shRNA}$-Exos (**Fig. 6G-H**). In $USCs^{shDMBT1\ \#1}$-Exos-treated wounds, the numbers of proliferating skin cells were lower when compared with the $USCs^{Con\ shRNA}$-Exos group (**Fig. 6G-H**). These data indicate that DMBT1 mediates, at least in part, the USC-Exos-induced pro-wound healing effects.

## Exosomal DMBT1 promotes angiogenesis in the wound sites of diabetic mice

We then evaluated the role of exosomal DMBT1 in angiogenesis in diabetic mice. Skin images from the undersurface revealed that $USCs^{Con\ shRNA}$-Exos-treated wounds exhibited much more newly formed blood vessels compared with the control wounds at day 12

post-wounding, whereas the pro-angiogenic effect of USCs$^{shDMBT1\ \#1}$-Exos was lower than that in the USCs$^{Con\ shRNA}$-Exos group (**Fig. 7A**). Dermal microvessels were immunostained for the endothelial marker CD31. As shown in **Fig. 7B**, a larger amount of blood vessels were observed in USCs$^{Con\ shRNA}$-Exos-treated wounds as compared to the wounds treated with exosomes diluents (PBS), but no significant positive effect on blood vessel formation was observed in the USCs$^{shDMBT1\ \#1}$-Exos group. Quantitative analysis of the density of new blood vessels, defined as the number of CD31-positive cells per mm$^2$, confirmed that DMBT1 expression in USC-Exos was important for the beneficial effect of USC-Exos on revascularization of the diabetic wounds (**Fig. 7C**). Taken together, our data suggest that DMBT1 is essential for the USC-Exos-induced promotion of angiogenesis in diabetic mice.

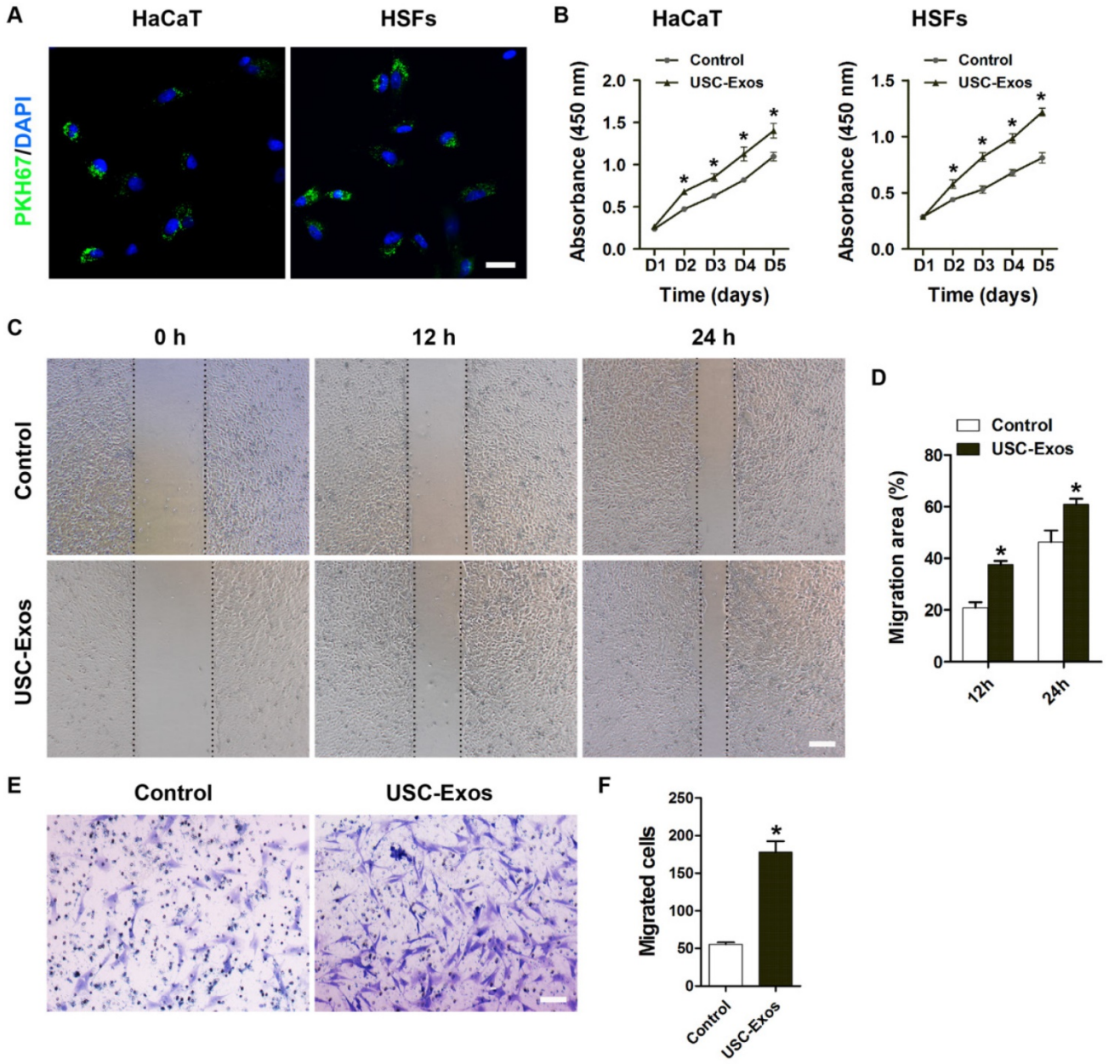


**Figure 2. USC-Exos enhance the proliferation and migration of keratinocytes and fibroblasts. (A)** Fluorescence microscopy analysis of PKH67-labeled USC-Exos internalization by human keratinocytes cell line HaCaT and skin fibroblasts (HSFs). The green-labeled exosomes were visible in the perinuclear region of recipient cells. Scale bar: 50 μm. **(B)** The proliferation of HaCaT and HSFs receiving different treatments was tested by CCK-8 analysis. n = 4 per group. **(C)** Representative images of scratch wound assay in HaCaT treated with USC-Exos or PBS. Scale bar: 250 μm. **(D)** Quantitative analysis of the migration rates in (C). n = 3 per group. **(E)** The migration of HSFs stimulated by USC-Exos or an equal volume of PBS was detected by the transwell assay. Scale bar: 100 μm. **(F)** Quantitative analysis of the migrated cells in (E). n = 3 per group. *$P$ < 0.05 vs. PBS (control) group.

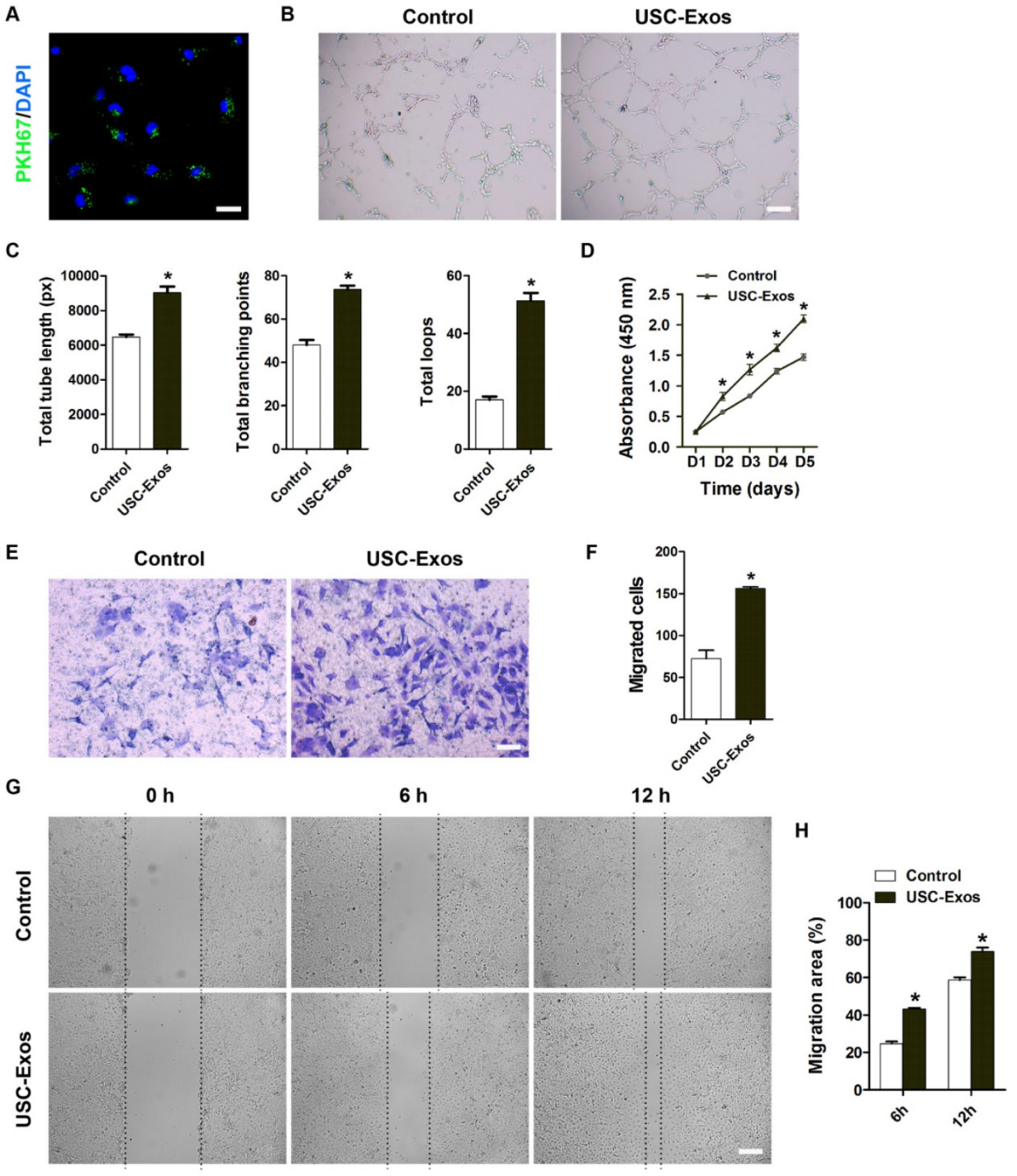


**Figure 3. USC-Exos augment the angiogenic activities of endothelial cells. (A)** Fluorescence microscopy analysis revealed that PKH67-labeled USC-Exos were incorporated into human microvascular endothelial cells (HMECs). Scale bar: 50 μm. **(B)** Representative images of the tube formation assay on Matrigel in HMECs treated with USC-Exos or PBS. Scale bar: 200 μm. (**C**) Quantitative analyses of the total tube length, total branching points and total loops in (B). n = 3 per group. **(D)** HMECs exhibited a much stronger proliferative ability when exposed to USC-Exos, as tested by CCK-8 analysis. n = 4 per group. Transwell assay **(E-F)** and scratch wound healing assay **(G-H)** revealed that USC-Exos up-regulated the motility of HMECs. Scale bar: 100 μm (E) or 250 μm (G). n = 3 per group. **P* < 0.05 vs. PBS (control) group.

## Discussion

In patients with diabetes mellitus, acute skin wounds resulting from trauma often become chronic non-healing wounds [3]. Numerous attempts have been made to accelerate the diabetic wound healing process, but optimal therapeutic strategies are still being developed [8]. In this study, we found that USC-Exos could effectively enhance the proliferation and migration of wound healing-related cells

(including keratinocytes, fibroblasts and vascular endothelial cells), as well as the angiogenic tube formation of endothelial cells. Results of proteomic analysis revealed that USC-Exos were enriched in the proteins that are involved in regulation of wound healing-related biological processes. Particularly, a pro-angiogenic protein DMBT1 was extremely highly expressed in USC-Exos and further functional assays showed that DMBT1 was required for USC-Exos-induced promotion of angiogenic responses of endothelial cells. *In vivo*, we found that the topical treatment of USC-Exos could promote angiogenesis and wound healing in STZ-induced diabetic mice, whereas these effects were markedly attenuated with the inhibition of DMBT1 expression in USCs-Exos. Our results suggest that USC-Exos may transfer DMBT1 protein to resident endothelial cells to evoke their regenerative responses, thereby accelerating revascularization and cutaneous wound healing.

Exosomes-based cell-free therapy represents an attractive approach for tissue engineering, due to their advantages of non-immune rejection, non-tumorigenicity, high stability, ease of reaching the wound sites and no vascular obstructive concern [31-34]. To our knowledge, this study is the first to show that the local transplantation of USC-Exos into full-thickness excisional skin wounds in diabetic mice was able to induce prominent regenerative effects, as defined by a more rapid wound closure, higher rates of re-epithelialization, collagen deposition and skin cell proliferation, as well as less scar formation. New vessel formation in postnatal life occurs mainly via angiogenesis, which provides oxygen and nutrients to the wounds for sustaining the proliferation of skin cells, re-epithelialization and collagen synthesis [35, 36]. However, angiogenesis frequently gets compromised in diabetics, which consequently leads to delayed wound healing [8, 37]. Herein, we found that USC-Exos markedly enhanced the amount of newly formed blood vessels in the diabetic wounds. *In vitro* functional assays revealed that USC-Exos increased the angiogenic activities of endothelial cells. The results suggest that the pro-wound healing action of USC-Exos is likely attributable to their stimulatory effects on endothelial angiogenesis.

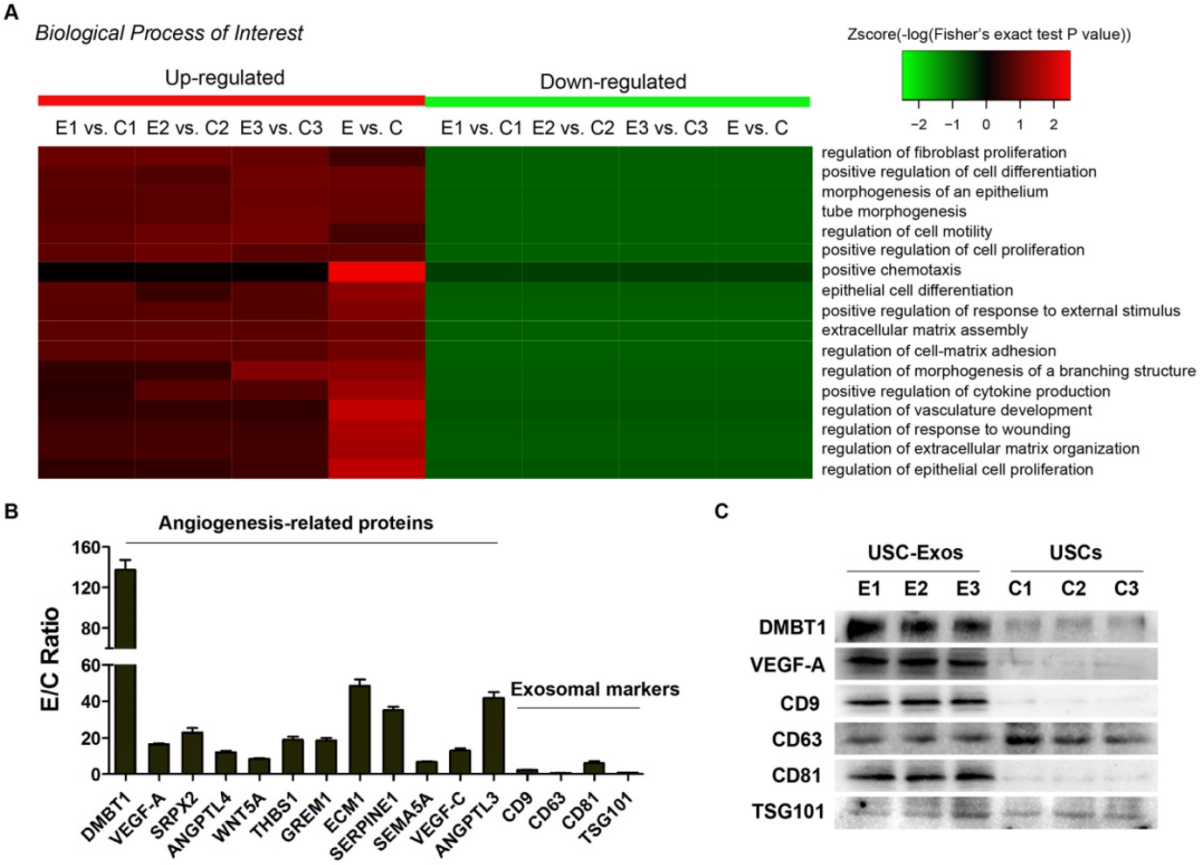


**Figure 4. Proteomic analysis of USCs and USC-Exos.** The differentially expressed proteins (a cutoff of absolute fold change ≥ 1.5 and *p* value < 0.05) in USC-Exos compared with USCs were categorized according to the biological process (GO term) they are involved in. A series of wound healing-related biological processes are shown in **(A)**. n = 3 per group. **(B)** The ratio of expression of a class of angiogenesis-related proteins and exosomal markers in USC-Exos compared to that in USCs. n = 3 per group. **(C)** The protein levels of DMBT1, VEGF-A and a series of exosomal markers in USC-Exos and USCs were verified by western blotting. n = 3 per group. *P < 0.05 vs. USCs group.

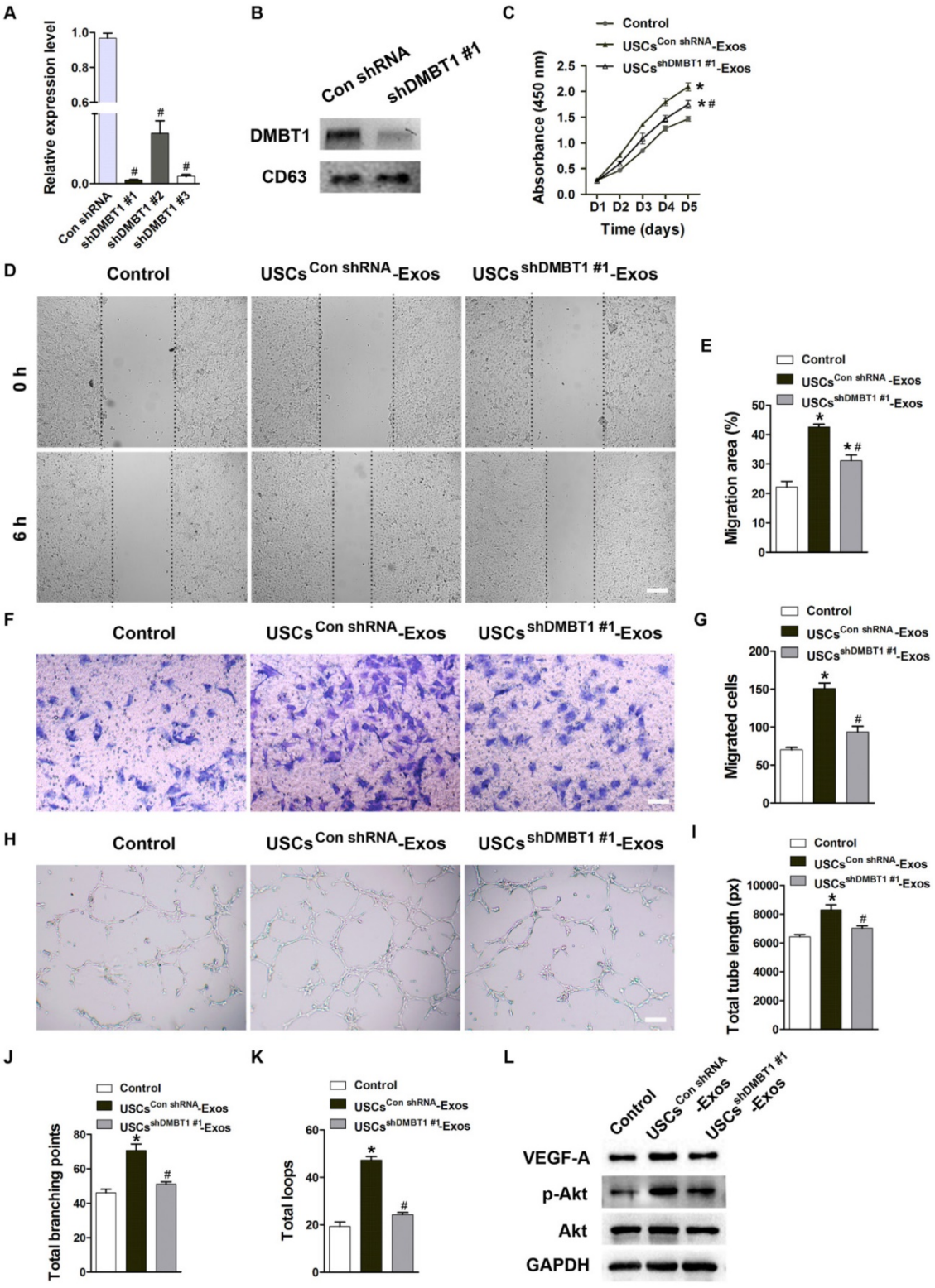


**Figure 5. DMBT1 mediates the pro-angiogenic effects of USC-Exos on endothelial cells. (A)** The inhibitory efficiency of shRNAs targeting DMBT1 was verified by qRT-PCR analysis. n = 3 per group. #*P* < 0.05 vs. Con shRNA group. **(B)** Western blot analysis of DMBT1 in exosomes from DMBT1-silenced USCs (USCs$^{shDMBT1\ \#1}$-Exos) and from Con shRNA-treated USCs (USCs$^{Con\ shRNA}$-Exos). **(C)** The proliferation of HMECs treated with PBS, USCs$^{Con\ shRNA}$-Exos and USCs$^{shDMBT1\ \#1}$-Exos was tested by CCK-8 analysis. n = 4 per group. **(D-G)** The migration of HMECs stimulated by PBS, USCs$^{Con\ shRNA}$-Exos and USCs$^{shDMBT1\ \#1}$-Exos was detected by the scratch wound assay **(D-E)** (Scale bar: 250 μm) and the transwell assay **(F-G)** (Scale bar: 100 μm). n = 3 per group. **(H)** Representative images of the tube formation assay in HMECs treated with PBS, USCs$^{Con\ shRNA}$-Exos and USCs$^{shDMBT1\ \#1}$-Exos. Scale bar: 200 μm. (**I-K**) Quantitative analyses of the total tube length, total branching points and total loops in (H). n = 3 per group. (**L**) Detection of the protein levels of VEGF-A, Akt and p-Akt in HMECs receiving different treatments by western blotting. n = 3 per group. **P* < 0.05 vs. PBS (control) group, #*P* < 0.05 vs. USCs$^{Con\ shRNA}$-Exos group.

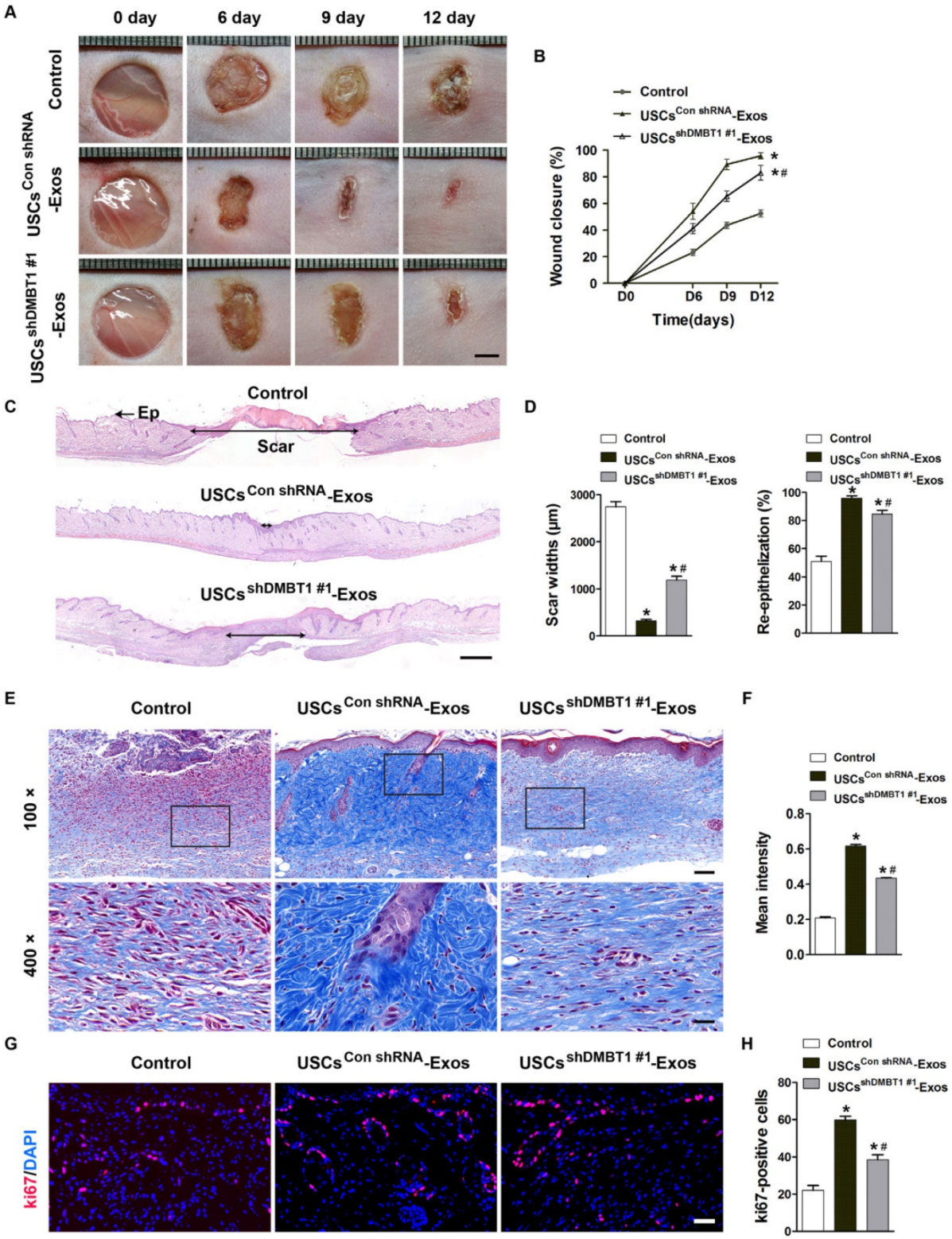


**Figure 6. Exosomal DMBT1 accelerates cutaneous wound healing in diabetic mice. (A)** Gross view of wounds treated with PBS, USCs$^{Con\ shRNA}$-Exos and USCs$^{shDMBT1\ \#1}$-Exos at days 6, 9 and 12 post-wounding. Scale bar: 2 mm. **(B)** The rate of wound-closure in wounds receiving different treatments at the indicated times. n = 8 per group. **(C)** H&E staining of wound sections treated with PBS, USCs$^{Con\ shRNA}$-Exos and USCs$^{shDMBT1\ \#1}$-Exos at 12 days after operation. The double-headed black arrows indicate the edges of the scars. Ep: epithelium. Scale bar: 500 μm. **(D)** Quantitative analysis of scar widths and the extent of re-epithelialization in (C). n = 6 per group. **(E)** Masson's trichrome staining of wound sections treated with PBS, USCs$^{Con\ shRNA}$-Exos and USCs$^{shDMBT1\ \#1}$-Exos. n = 3 per group. Scale bar: 100 μm (top) or 25 μm (bottom). **(F)** Quantitative analysis of the mean intensity of Masson-stained areas in (E). n = 3 per group. **(G)** Representative images of ki67 staining of wound sections treated with PBS, USCs$^{Con\ shRNA}$-Exos and USCs$^{shDMBT1\ \#1}$-Exos. Scale bar: 50 μm. **(H)** Quantification of the number of ki67-positive cells in (F). n = 6 per group. *$P$ < 0.05 vs. PBS (control) group, #$P$ < 0.05 vs. USCs$^{Con\ shRNA}$-Exos group.

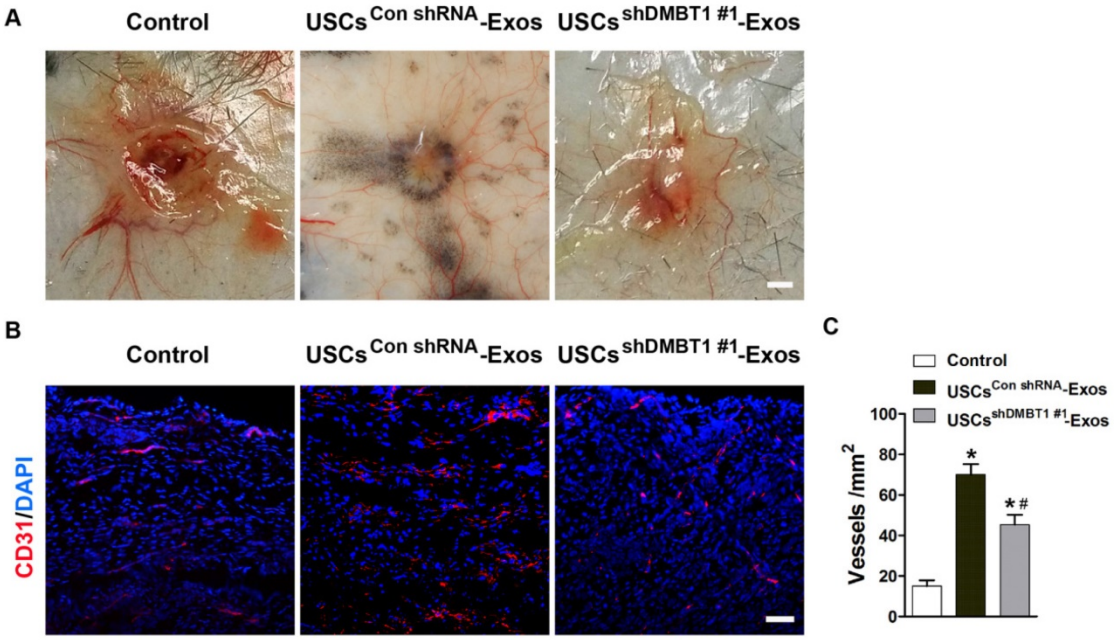


**Figure 7. Exosomal DMBT1 promotes angiogenesis in the wound sites of diabetic mice. (A)** Gross view of wounds treated with PBS, USCs$^{Con\ shRNA}$-Exos and USCs$^{shDMBT1\ \#1}$-Exos at day 12 post-wounding from the undersurface. Newly formed blood vessels were detected in the wound sites. Scale bar: 2 mm. **(B)** CD31 immunofluorescence staining of wound sections treated with PBS, USCs$^{Con\ shRNA}$-Exos and USCs$^{shDMBT1\ \#1}$-Exos at day 12 post-wounding. Scale bar: 50 μm. **(C)** Quantitative analysis of the density of blood vessels in (B). n = 6 per group. *$P$ < 0.05 vs. PBS (control) group, #$P$ < 0.05 vs. USCs$^{Con\ shRNA}$-Exos group.

In the process of wound healing, keratinocytes and fibroblasts also play important roles, keratinocytes in the re-epithelization process and fibroblasts in the process of collagen synthesis and wound contraction [38-40]. The loss of functional dermal extracellular matrix is one of the major features of chronic wounds [41]. Fibroblasts can secrete structural extracellular matrix proteins such as various types of collagens, which they can deposit and remodel in the wound sites to restore tissue integrity [42, 43]. Although no *in vivo* data directly showed the effects of USC-Exos on the functional properties of fibroblasts and keratinocytes in our study, we found that transplantation of USC-Exos facilitated skin cell proliferation and collagen deposition in the diabetic wounds. *In vitro* assays revealed that USC-Exos could be taken up by keratinocytes and fibroblasts, and increase their abilities to proliferate and migrate. Thus, in addition to promoting angiogenesis, the pro-wound healing effects of USC-Exos may also be mediated by the direct activation of keratinocytes and fibroblasts. Proteomic data showed that USC-Exos contained abundant proteins that are implicated in the modulation of skin cell proliferation and motility, extracellular matrix assembly and organization, and cell−matrix adhesion, which was consistent with their function properties. However, the proteins through which USC-Exos exert direct effects on keratinocytes and fibroblasts still need further investigation. Another limitation of our study is that the specific molecular mechanism by which USC-Exos are internalized by recipient cells was not assessed.

DMBT1, also referred to as salivary agglutinin (SAG), gp-340, muclin or hensin, is a secreted epithelial glycoprotein expressed in the gastrointestinal system, salivary glands, lung, kidney, liver, epidermis, etc [44]. Among the many proposed functions of the protein, those that have been most investigated are as a tumor suppressor [45], as a regulator of epithelial functional differentiation [46], as a Golgi cargo receptor in the regulated secretory pathway [47], as a component of the innate immune defenses against bacterial pathogens [48] and as a protector of intestinal mucosa [49]. Recently, DMBT1 has been reported to function in angiogenesis by promoting proliferation, migration and adhesion of endothelial cells, as well as vascular repair in hindlimb ischemia mouse models [50]. DMBT1 may also be able to induce angiogenic responses in alveolar tissues by promoting VEGF-A production [29]. These findings reveal that DMBT1 may facilitate diabetic wound angiogenesis and thereby promote the healing of wounds.

Exosomes represent an important mode of cell-to-cell communication, as they can serve as vehicles to transfer bioactive lipids, nucleic acids and proteins between cells to elicit biological responses in recipient cells [5]. For example, Choi et al. showed that exosomes from differentiating human skeletal muscle cells shuttle various muscle development-related proteins and can increase the regeneration of

myofibers in injured skeletal muscle [51]. Zhang et al. reported that exosomes from human umbilical cord-derived MSCs can induce β-catenin nuclear translocation and enhance the activity of recipient skin cells by transferring Wnt4 protein [11]. In our study, we found that DMBT1 was extremely highly expressed in USC-Exos, as evidenced by the proteomic data and western blotting results. When DMBT1 was inhibited in the parent cell USCs, the positive effects of USC-Exos on endothelial cell function *in vitro*, angiogenesis and diabetic wound healing *in vivo* were all markedly suppressed. Studies have revealed that VEGF-A and PI3K-Akt signaling are the downstream targets of DMBT1 [29, 30]. In accord with these findings, results of our study showed that the DMBT1-enriched USC-Exos could induce significant increases in the protein levels of VEGF-A and phosphorylation of Akt (an indicator of PI3K activation). However, the effects were compromised once DMBT1 expression in USC-Exos was inhibited. Our results suggest that DMBT1 is a critical mediator in USC-Exos-induced regulation of endothelial angiogenesis and diabetic wound healing. It should be noted that the effects of USC-Exos on angiogenesis and wound healing *in vitro* and *in vivo* were not entirely abolished by DMBT1 inhibition, suggesting that other signaling molecules are also be involved in these processes. This was consistent with our proteomic data showing that USC-Exos were also enriched in the pro-angiogenic proteins such as VEGFA, SRPX2, ANGPTL4, etc. Thus, the pro-angiogenic and -wound healing effects of USC-Exos were mediated by the transfer of multiple functional molecules, instead of via a single angiogenic factor.

## Conclusions

In summary, our findings demonstrate that USC-Exos can effectively augment the functional properties of skin cells and accelerate diabetic wound healing in mice. In the process of USC-Exos-dependent regulation of angiogenesis and diabetic wound healing, DMBT1 plays a crucial role, as the pro-angiogenic and -wound healing effects of USC-Exos can be attenuated by inhibition of DMBT1 expression in USCs. Our findings suggest that USC-Exos may represent a promising strategy for diabetic wound healing by promoting angiogenesis via transferring DMBT1 protein.

## Abbreviations

USCs: urine-derived stem cells; USC-Exos: exosomes from urine-derived stem cells; DMBT1: deleted in malignant brain tumors 1; MVBs: multivesicular bodies; MSCs: mesenchymal stem cells; PBS: phosphate-buffered saline; FBS: fetal bovine serum; ARS: alizarin red S; TEAB: tetra-ethylammonium bromide; MS: mass spectrometry; GO: gene ontology; HaCaT: a human skin keratinocyte cell line; HSFs: human skin fibroblasts; HMECs: human microvascular endothelial cells; CCK-8: cell counting kit-8; qRT-PCR: quantitative real-time PCR; VEGF-A: vascular endothelial growth factor A; p-Akt: phosphorylate Akt; STZ: strepto-zotocin; H&E: hematoxylin and eosin.

## Acknowledgements

This work was supported by the Thousand Youth Talents Plan of China (Grant No. D1119003), the Excellent Young Scientist Award of National Natural Science Foundation of China (Grant No. 81522012), the National Natural Science Foundation of China (Grant No. 81670807, 81702237, 81600699, 81701383, 81370974), the Hunan Youth Talent Project (Grant No. 2016RS3021), the Innovation Driven Project of Central South University (2016CX028), the Youth Foundation of Xiangya Hospital in Central South University (Grant No. 2016Q10), the Fundamental Research Funds for the Central Universities of Central South University (Grant No. 2017zzts032, 2017zzts014), the Hunan Province Natural Science Foundation of China (Grant No. 2017JJ3501), the China Postdoctoral Science Foundation (Grant No. 2017M612596) and the Natural Science Foundation for Distinguished Yong Scholars of Guangdong Province (2016A030306051).

### Author contributions

HX and CYC conceived and designed the experiments. SSR, CYC, LR, XKH, YJT, YH and JL performed the experiments. SSR and CYC analysed the data and prepared all the figures. JC, ZXW, ZZL, HML, SYT and RX provided technical support. CYC, HY and JH provided the urine samples. HX and CYC wrote the manuscript. All authors reviewed and agreed the manuscript.

## Supplementary Material

All proteins identified and quantified by proteomic analysis are listed in **Table S1**.
http://www.thno.org/v08p1607s1.xlsx

The differentially expressed proteins between USC-Exos and USCs were biologically interpreted and their involved biological processes are shown in **Fig. S1**. http://www.thno.org/v08p1607s2.pdf

## Competing Interests

The authors have declared that no competing interest exists.

## References


1. van Zanten MC, Mistry RM, Suami H, Campbell-Lloyd A, Finkemeyer JP, Piller NB, et al. The Lymphatic Response to Injury with Soft-Tissue Reconstruction in High-Energy Open Tibial Fractures of the Lower Extremity. Plast Reconstr Surg. 2017; 139: 483-91.
2. Bhandari M, Petrisor BA, Jeray KJ. Wound Irrigation in Initial Management of Open Fractures. N Engl J Med. 2016; 374: 1789-90.
3. Falanga V. Wound healing and its impairment in the diabetic foot. Lancet. 2005; 366: 1736-43.
4. Ackermann M, Pabst AM, Houdek JP, Ziebart T, Konerding MA. Priming with proangiogenic growth factors and endothelial progenitor cells improves revascularization in linear diabetic wounds. Int J Mol Med. 2014; 33: 833-9.
5. Tkach M, Thery C. Communication by Extracellular Vesicles: Where We Are and Where We Need to Go. Cell. 2016; 164: 1226-32.
6. Au Yeung CL, Co NN, Tsuruga T, Yeung TL, Kwan SY, Leung CS, et al. Exosomal transfer of stroma-derived miR21 confers paclitaxel resistance in ovarian cancer cells through targeting APAF1. Nat Commun. 2016; 7: 11150.
7. Jiang N, Xiang L, He L, Yang G, Zheng J, Wang C, et al. Exosomes Mediate Epithelium-Mesenchyme Crosstalk in Organ Development. ACS Nano. 2017; 11: 7736-46.
8. Zhang J, Chen C, Hu B, Niu X, Liu X, Zhang G, et al. Exosomes Derived from Human Endothelial Progenitor Cells Accelerate Cutaneous Wound Healing by Promoting Angiogenesis Through Erk1/2 Signaling. Int J Biol Sci. 2016; 12: 1472-87.
9. Basu J, Ludlow JW. Exosomes for repair, regeneration and rejuvenation. Expert Opin Biol Ther. 2016: 1-18.
10. Hu L, Wang J, Zhou X, Xiong Z, Zhao J, Yu R, et al. Exosomes derived from human adipose mensenchymal stem cells accelerates cutaneous wound healing via optimizing the characteristics of fibroblasts. Sci Rep. 2016; 6: 32993.
11. Zhang B, Wang M, Gong A, Zhang X, Wu X, Zhu Y, et al. HucMSC-Exosome Mediated-Wnt4 Signaling Is Required for Cutaneous Wound Healing. Stem cells. 2015; 33: 2158-68.
12. Zhang B, Wu X, Zhang X, Sun Y, Yan Y, Shi H, et al. Human umbilical cord mesenchymal stem cell exosomes enhance angiogenesis through the Wnt4/beta-catenin pathway. Stem Cells Transl Med. 2015; 4: 513-22.
13. Zhang Y, McNeill E, Tian H, Soker S, Andersson KE, Yoo JJ, et al. Urine derived cells are a potential source for urological tissue reconstruction. J Urol. 2008; 180: 2226-33.
14. Zhang D, Wei G, Li P, Zhou X, Zhang Y. Urine-derived stem cells: A novel and versatile progenitor source for cell-based therapy and regenerative medicine. Genes Dis. 2014; 1: 8-17.
15. Bharadwaj S, Liu G, Shi Y, Wu R, Yang B, He T, et al. Multipotential differentiation of human urine-derived stem cells: potential for therapeutic applications in urology. Stem cells. 2013; 31: 1840-56.
16. Chun SY, Kim HT, Lee JS, Kim MJ, Kim BS, Kim BW, et al. Characterization of urine-derived cells from upper urinary tract in patients with bladder cancer. Urology. 2012; 79: 1186 e1-7.
17. Fu Y, Guan J, Guo S, Guo F, Niu X, Liu Q, et al. Human urine-derived stem cells in combination with polycaprolactone/gelatin nanofibrous membranes enhance wound healing by promoting angiogenesis. J Transl Med. 2014; 12: 274.
18. Zhou T, Benda C, Dunzinger S, Huang Y, Ho JC, Yang J, et al. Generation of human induced pluripotent stem cells from urine samples. Nat Protoc. 2012; 7: 2080-9.
19. Tao SC, Yuan T, Zhang YL, Yin WJ, Guo SC, Zhang CQ. Exosomes derived from miR-140-5p-overexpressing human synovial mesenchymal stem cells enhance cartilage tissue regeneration and prevent osteoarthritis of the knee in a rat model. Theranostics. 2017; 7: 180-95.
20. Thery C, Amigorena S, Raposo G, Clayton A. Isolation and characterization of exosomes from cell culture supernatants and biological fluids. Curr Protoc Cell Biol 2006, Chapter 3, Unit 3.22, pp 1-29.
21. Melo SA, Luecke LB, Kahlert C, Fernandez AF, Gammon ST, Kaye J, et al. Glypican-1 identifies cancer exosomes and detects early pancreatic cancer. Nature. 2015; 523: 177-82.
22. Xie H, Cui Z, Wang L, Xia Z, Hu Y, Xian L, et al. PDGF-BB secreted by preosteoclasts induces angiogenesis during coupling with osteogenesis. Nat Med. 2014; 20: 1270-8.
23. Yan W, Tu B, Liu YY, Wang TY, Qiao H, Zhai ZJ, et al. Suppressive Effects of Plumbagin on Invasion and Migration of Breast Cancer Cells via the Inhibition of STAT3 Signaling and Down-regulation of Inflammatory Cytokine Expressions. Bone Res. 2013; 1: 362-70.
24. Su ST, Yeh CL, Hou YC, Pai MH, Yeh SL. Dietary glutamine supplementation enhances endothelial progenitor cell mobilization in streptozotocin-induced diabetic mice subjected to limb ischemia. J Nutr Biochem. 2017; 40: 86-94.
25. Carr MJ, Li Y, Rezakhanlou AM, Ghahary A. Keratinocyte-Releasable Factors Stimulate the Expression of Granulocyte Colony-Stimulating Factor in Human Dermal Fibroblasts. J Cell Biochem. 2017; 118: 308-17.
26. Li Q, Hu B, Hu GW, Chen CY, Niu X, Liu J, et al. tRNA-Derived Small Non-Coding RNAs in Response to Ischemia Inhibit Angiogenesis. Sci Rep. 2016; 6: 20850.
27. Kusumbe AP, Ramasamy SK, Adams RH. Coupling of angiogenesis and osteogenesis by a specific vessel subtype in bone. Nature. 2014; 507: 323-8.
28. Yu X, Li W, Deng Q, You S, Liu H, Peng S, et al. Neoalbaconol inhibits angiogenesis and tumor growth by suppressing EGFR-mediated VEGF production. Mol Carcinog. 2017; 56: 1414-26.
29. Muller H, Nagel C, Weiss C, Mollenhauer J, Poeschl J. Deleted in malignant brain tumors 1 (DMBT1) elicits increased VEGF and decreased IL-6 production in type II lung epithelial cells. BMC Pulm Med. 2015; 15: 32.
30. Shen S, Liu H, Wang Y, Wang J, Ni X, Ai Z, et al. Long non-coding RNA CRNDE promotes gallbladder carcinoma carcinogenesis and as a scaffold of DMBT1 and C-IAP1 complexes to activating PI3K-AKT pathway. Oncotarget. 2016; 7: 72833-44.
31. Xin H, Li Y, Chopp M. Exosomes/miRNAs as mediating cell-based therapy of stroke. Front Cell Neurosci. 2014; 8: 377.
32. De Jong OG, Van Balkom BW, Schiffelers RM, Bouten CV, Verhaar MC. Extracellular vesicles: potential roles in regenerative medicine. Front Immunol. 2014; 5: 608.
33. Burger D, Vinas JL, Akbari S, Dehak H, Knoll W, Gutsol A, et al. Human endothelial colony-forming cells protect against acute kidney injury: role of exosomes. Am J Pathol. 2015; 185: 2309-23.
34. Rani S, Ritter T. The Exosome - A Naturally Secreted Nanoparticle and its Application to Wound Healing. Adv Mater. 2016; 28: 5542-52.
35. Kant V, Gopal A, Kumar D, Pathak NN, Ram M, Jangir BL, et al. Curcumin-induced angiogenesis hastens wound healing in diabetic rats. J Surg Res. 2015; 193: 978-88.
36. Zhou J, Zhang X, Liang P, Ren L, Zeng J, Zhang M, et al. Protective role of microRNA-29a in denatured dermis and skin fibroblast cells after thermal injury. Biol Open. 2016; 5: 211-9.
37. Liu F, Chen DD, Sun X, Xie HH, Yuan H, Jia W, et al. Hydrogen sulfide improves wound healing via restoration of endothelial progenitor cell functions and activation of angiopoietin-1 in type 2 diabetes. Diabetes. 2014; 63: 1763-78.
38. Souren JM, Ponec M, van Wijk R. Contraction of collagen by human fibroblasts and keratinocytes. In Vitro Cell Dev Biol. 1989; 25: 1039-45.
39. Brem H, Tomic-Canic M. Cellular and molecular basis of wound healing in diabetes. J Clin Invest. 2007; 117: 1219-22.
40. Driskell RR, Lichtenberger BM, Hoste E, Kretzschmar K, Simons BD, Charalambous M, et al. Distinct fibroblast lineages determine dermal architecture in skin development and repair. Nature. 2013; 504: 277-81.
41. Schultz GS, Wysocki A. Interactions between extracellular matrix and growth factors in wound healing. Wound Repair Regen. 2009; 17: 153-62.
42. Hodde JP, Johnson CE. Extracellular matrix as a strategy for treating chronic wounds. Am J Clin Dermatol. 2007; 8: 61-6.
43. Liu J, Luo C, Yin Z, Li P, Wang S, Chen J, et al. Downregulation of let-7b promotes COL1A1 and COL1A2 expression in dermis and skin fibroblasts during heat wound repair. Mol Med Rep. 2016; 13: 2683-8.
44. De Lisle RC, Xu W, Roe BA, Ziemer D. Effects of Muclin (Dmbt1) deficiency on the gastrointestinal system. Am J Physiol Gastrointest Liver Physiol. 2008; 294: G717-27.
45. Ligtenberg AJ, Veerman EC, Nieuw Amerongen AV, Mollenhauer J. Salivary agglutinin/ glycoprotein-340/DMBT1: a single molecule with variable composition and with different functions in infection, inflammation and cancer. Biol Chem. 2007; 388: 1275-89.
46. Al-Awqati Q. Terminal differentiation in epithelia: the role of integrins in hensin polymerization. Annu Rev Physiol. 2011; 73: 401-12.
47. De Lisle RC, Norkina O, Roach E, Ziemer D. Expression of pro-Muclin in pancreatic AR42J cells induces functional regulated secretory granules. Am J Physiol Cell Physiol. 2005; 289: C1169-78.
48. Li J, Metruccio MME, Evans DJ, Fleiszig SMJ. Mucosal fluid glycoprotein DMBT1 suppresses twitching motility and virulence of the opportunistic pathogen Pseudomonas aeruginosa. PLoS Pathog. 2017; 13: e1006392.
49. Renner M, Bergmann G, Krebs I, End C, Lyer S, Hilberg F, et al. DMBT1 confers mucosal protection in vivo and a deletion variant is associated with Crohn's disease. Gastroenterology. 2007; 133: 1499-509.
50. Muller H, Hu J, Popp R, Schmidt MH, Muller-Decker K, Mollenhauer J, et al. Deleted in malignant brain tumors 1 is present in the vascular extracellular matrix and promotes angiogenesis. Arterioscler Thromb Vasc Biol. 2012; 32: 442-8.
51. Choi JS, Yoon HI, Lee KS, Choi YC, Yang SH, Kim IS, et al. Exosomes from differentiating human skeletal muscle cells trigger myogenesis of stem cells and provide biochemical cues for skeletal muscle regeneration. J Control Release. 2016; 222: 107-15.